

Supplementary Information

Durable and efficient BTC-assisted 2D/0D of Al-Ni-MOF nanostructures for modern electrochemical energy systems

Xiaolong Leng^{a,#}, S. V. Prabhakar Vattikuti^{b,#}, Mohan Rao Tamtam^{c,*}, Jaesool Shim^{a,*}, Huynh Thanh Liem^{d,e,*}, Nam Nguyen Dang^{d,e}

^aSchool of Mechanical Engineering, Hubei Engineering University, Xiaogan 432000, China.

^bSchool of Mechanical Engineering, College of Engineering, Yeungnam University, Gyeongsan 38541, Republic of Korea.

^cSchool of Computer Science and Engineering, College of Digital Convergence, Yeungnam University, Gyeongsan 38541, Republic of Korea.

^dFuture Materials & Devices Lab., Institute of Fundamental and Applied Sciences, Duy Tan University, Ho Chi Minh City 70000, Viet Nam.

^eThe Faculty of Environmental and Chemical Engineering, Duy Tan University, Danang 50000, Viet Nam.

*E-mail: mohanrtam@gmail.com, jshim@ynu.ac.kr, huynhthanhliem@duytan.edu.vn

Authors equally contributed

1.1 Characterization

X-ray diffraction (XRD; PANalytical) experiments were conducted using programmable PANalytical X-ray generator operated at 40 kV and 40 mA. Scanning electron microscopy (SEM; Hitachi-S-4800) was employed to observe the surface morphologies of the catalysts. High-resolution transmission electron microscopy (HRTEM; Tecnai G2 F20 S-Twin) was performed to examine the nanocrystal shape and size. Energy-dispersive X-ray (EDX)-HRTEM was employed to distinguish the individual elements. X-ray photoelectron spectroscopy (XPS; Thermo Scientific photoelectron spectrometer) was employed to define the surface states.

1.2 Electrochemical testing

All the electrochemical measurements were carried out on a Biologic Sp-200 electrochemical workstation with a standard three-electrode setup. As-synthesized samples were drop casted on Ni foam and used the working electrode. The Hg/HgO electrode and Platinum mesh were served as the reference electrode and the counter electrode, respectively. CV, galvanostatic charge-discharge (GCD), and EIS were used to assess the electrochemical activity of the electrodes. The CV tests were performed at several scan rates, ranging from 1 to 20 mV/s at a potential of 0 to 0.6 V. The GCD tests were executed within the range of 0 to 0.5 V versus Hg/HgO at various current densities (0.8-4 A/g). All the electrochemical experiments were performed on a Biologic SP-200 electrochemical workstation in a 1.0 M KOH solution.

Specific capacitance (C_s) from Galvanostatic charge-discharge can also be calculated as

$$C_s = \frac{I\Delta t}{m\Delta V} \quad (1)$$

where, ' I ' implies current intensity and ' Δt ' entails discharge time (t) of the experimental charge-discharge curve. To achieve the mass of active material on each electrode based on their respective capacitance and operating voltage window. The formula is:

$$m^+/m^- = (C^- \times \Delta V^-) / (C^+ \times \Delta V^+) \quad (2)$$

where, m^+ and m^- : Represent the mass of active material in the positive and negative electrodes,

respectively. C^+ and C^- : Represent the specific capacitance of the positive and negative electrodes, respectively. ΔV^+ and ΔV^- : Represent the potential window (voltage range) of the positive and negative electrodes, respectively. The optimal mass ratio of positive electrode to negative one was ~0.32.

Further specific energy (E) in Wh/kg associated with specific power (P) in W/kg of electrode were evaluated from the charge-discharge dimensions using the reckoning,

$$E = \frac{1}{2} \left[\frac{C_s \Delta V^2}{3.6} \right] \quad (3)$$

$$P = \frac{3600 \times E}{\Delta t} \quad (4)$$

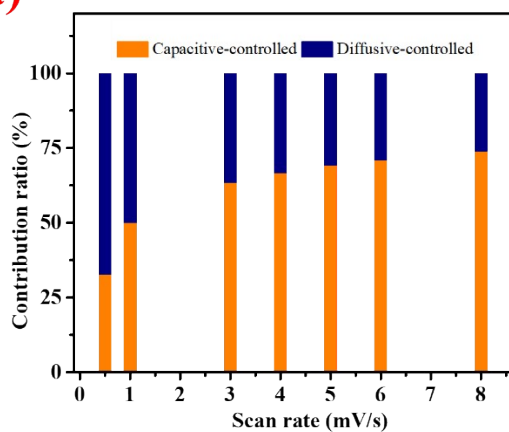
1.3 PVA-KOH gel electrolyte

In order to prepare the alkaline PVA/KOH gel electrolyte, 3 g of polyvinylalcohol was dissolved in 24 mL of pure deionized water at 90 °C with continuous and vigorous stirring to obtain a clear solution. After 1 h, we obtained a clear viscous solution. KOH (3 g) was liquefied in 6 mL deionized water and then dropped into the cleared PVA solution with continuous stirring until complete dissolution and the formation of a gel-like solution. Finally, the PVA/KOH gel electrolyte was cooled to room temperature for further use.

1.4 Asymmetric device preparation procedure (ADs)

For an aqueous asymmetric supercapacitor, the Al-Ni-MOF//AC was used as both positive and negative electrodes. The wide potential window of 0-1.6 V was applied for the two-electrode system and gel electrolyte was used as the electrolyte. The positive electrode (7 mg of active material, 2 mg of carbon black, and 1 mg of PVDF, paste was prepared and drop casted on 14 mm diameter of Ni foam. The paste was then coated on the respective electrodes, and heated at 80°C for 12 h.

(a)



(b)

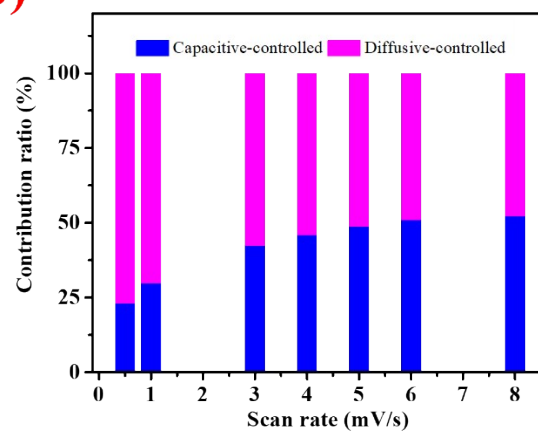


Fig. S1 Total contribution vs scan rate of (a) Al-MOF and (b) Ni-MOF electrodes.

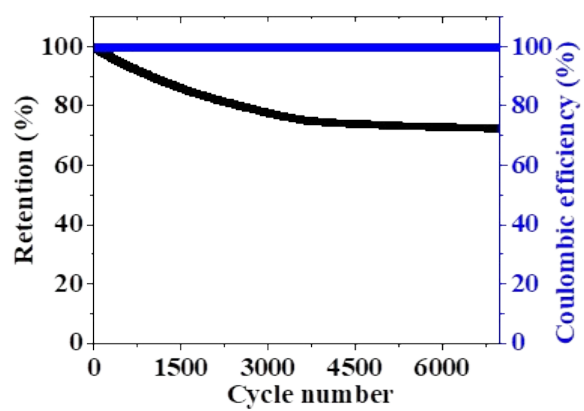


Fig. S2 Cycling stability and coulombic efficiency of the Al-Ni-MOF electrode.

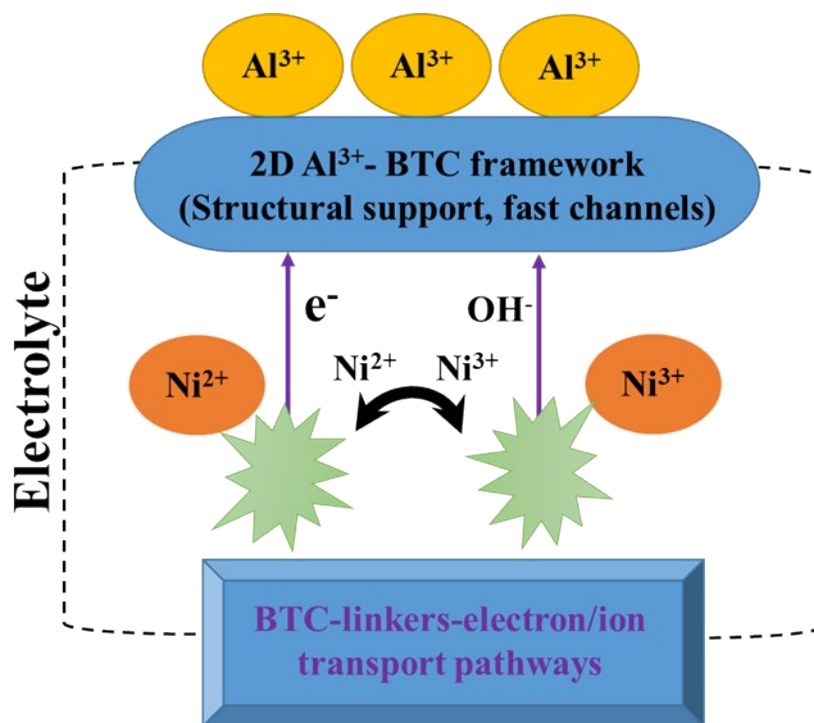


Fig. S3 Graphical representation of electrochemical storage mechanism of Al-Ni-MOF electrode.

Table: S1 Comparison of electrochemical activity of Al-Ni-MF electrode and other MOF-based electrodes in previous reports.

| Materials | Electrolyte | Scan rate or Current density | Sp. Capacitance (F/g) | References |
|--------------------------------|-------------------------------------|---------------------------------|-----------------------------|-------------|
| Mn-BDC MOF | 1M Na ₂ SO ₄ | 1 A/g | 178 | [1] |
| ZIF-8/PANI | 1 M H ₂ SO ₄ | 1 A/g | 236 | [2] |
| Co-Ni-MOF | 2 M KOH | 5 mA/cm ² | 43.6 F/cm ² | [3] |
| Cu MOF/rGO | PVA-Na ₂ SO ₄ | 1 A/g | 385 | [4] |
| UIO-66/rGO | 6 M KOH | 0.15 A/g | 302 | [5] |
| PANI-ZIF-67-CC | 3 M KCl | 10 mV/s | 21.46 mF/cm ² | [6] |
| ZIF-67/polyprrole nanotubes | 1M Na ₂ SO ₄ | 0.5 A/g | 597.6 | [7] |
| Ni-CoMOF | 3 M KOH | 1 A/g | 236.1 mAh/g | [8] |
| Al-MOF | 1 M KOH | 0.8 A/g | 112 F/g | [This work] |
| Al-Ni-MOF | 1 M KOH | 0.8 A/g | 1631.2 F/g | [This work] |

References:

- [1] Sundriyal, Shashank; Mishra, Sunita; Deep, Akash, Study of Manganese-1,4-Benzenedicarboxylate Metal Organic Framework Electrodes Based Solid State Symmetrical Supercapacitor, *Energy Procedia* (2019), 158, 5817-5824 CODEN: EPNRCV; ISSN:1876-6102. (Elsevier Ltd.).
- [2] Salunkhe, R. R.; Tang, J.; Kobayashi, N.; Kim, J.; Ide, Y.; Tominaka, S.; Kim, J. H.; Yamauchi, Y. Ultrahigh performance supercapacitors utilizing core-shell nanoarchitectures from a metalorganic framework-derived nanoporous carbon and a conducting polymer. *Chem. Sci.* 2016, 7, 5704–5713.
- [3] Jianying Liang, Shumin Qin, Shuang Luo, Yanru Wang, Jinglv Feng, Kang Liu , Shenna Liao, Zhenglong Xu, Jien Li, Epitaxially growing multilayer CoNi-MOFs nanosheets on activated carbon cloth for high-performance asymmetric supercapacitors, *Journal of Power Sources* 618 (2024) 235209.
- [4] Srimuk, P.; Luanwuthi, S.; Krittayavathananon, A.; Sawangphruk, M. Solid-type supercapacitor of reduced graphene oxide-metal organic framework composite coated on carbon fiber paper. *Electrochim. Acta* 2015, 157, 69–77.
- [5] Mao, M. L.; Sun, L. X.; Xu, F. Metal–Organic Frameworks/ Carboxyl Graphene Derived Porous Carbon as a Promising Supercapacitor Electrode Material. *Key Engineering Materials; Trans Tech Publ*, 2017; pp 756–763.
- [6] L. Wang, X. Feng, L. Ren, Q. Piao, J. Zhong, Y. Wang, H. Li, Y. Chen and B. Wang, *J. Am. Chem. Soc.*, 2015, 137, 4920–4923.
- [7] Xu, X.; Tang, J.; Qian, H.; Hou, S.; Bando, Y.; Hossain, M. S. A.; Pan, L.; Yamauchi, Y. Three-Dimensional Networked Metal- Organic Frameworks with Conductive Polypyrrole Tubes for Flexible Supercapacitors. *ACS Appl. Mater. Interfaces* 2017, 9, 38737–38744.
- [8] Y. Jiao, J. Pei, D. Chen, C. Yan, Y. Hu, Q. Zhang and G. Chen, Mixed-metallic MOF based electrode materials for high performance hybrid supercapacitors, *J. Mater. Chem. A*, 2017, 5, 1094–1102.